Supporting Information for ***Polymer Chemistry***

Electronic Supporting Information

Controllable synthesis of mussel-inspired catechol-formaldehyde resin microspheres and their silver-based nanohybrids for catalytic and antibacterial applications

Yu Yang,[a] Haixun Ji,[b] Haichao Duan,[a] Yuqin Fu[*, b], Siwen Xia[a] and Changli Lü[*, a]

[a] *Institute of Chemistry, Northeast Normal University, Changchun 130024, P. R. China*

[b] *College of Life Sciences, Jilin Agricultural University, Changchun 130118, P. R. China*

* Corresponding author.

E-mail addresses: lucl055@nenu.edu.cn (C. Lü); fuyuqin@jlau.edn.cn (Y.Q. Fu).

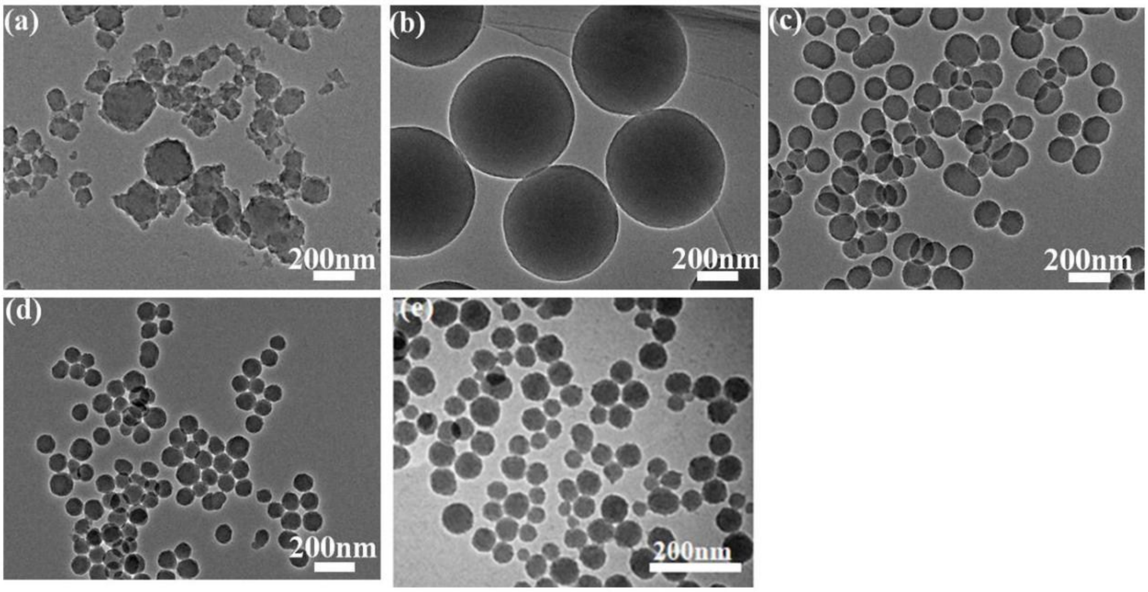

Fig. S1 TEM images of CFR nanospheres obtained from different amounts of ethanol and water: (a) 28 and 0 mL, (b) 24 and 4 mL, (c) 20 and 8 mL, (d) 12 and 16 mL, and (e) 0 and 28 mL, Reaction conditions: catechol 0.1 g, formaldehyde solution 0.14 mL, ammonia solution 0.15 mL, heating time 6 h, and reaction temperature 160 °C.

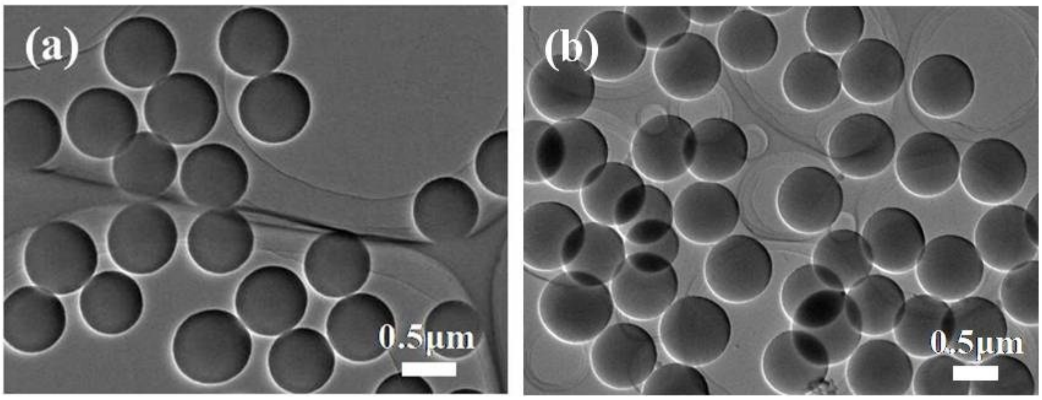

Fig. S2 TEM images of the CFR microspheres prepared with different amounts of ammonia solution: (a) 0.15 mL and (b) 0.3 mL. Reaction conditions: formaldehyde solution 0.14 mL, catechol 0.1 g, ethanol 20 mL, water 8 mL, heating time 6 h, and reaction temperature 160 °C.

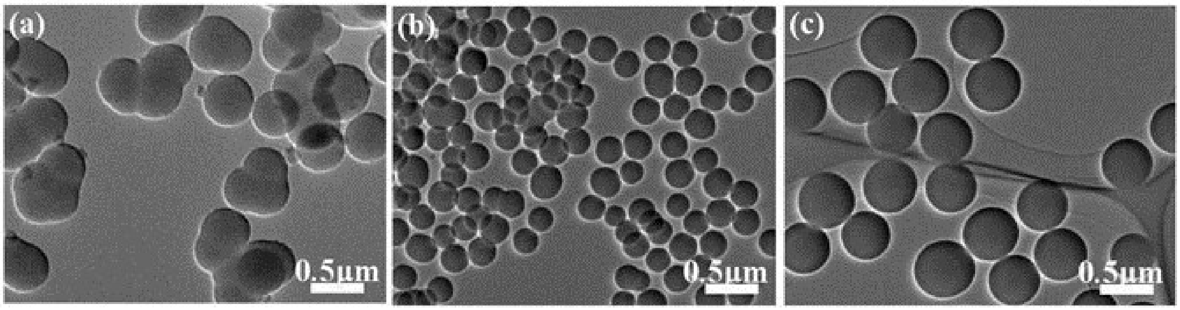

Fig. S3 TEM images of CFR nanospheres obtained from different temperature: (a) 120 °C, (b) 140 °C, and (c) 160 °C. Reaction conditions: catechol 0.1 g, formaldehyde solution 0.14 mL, ammonia solution 0.15 mL, ethanol 20 mL, water 8 mL, heating time 6 h.

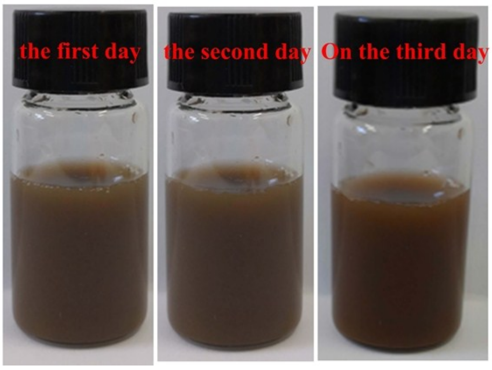

Fig. S4 Pictures of the dispersibility and stability of CFR nanospheres in an aqueous solution.

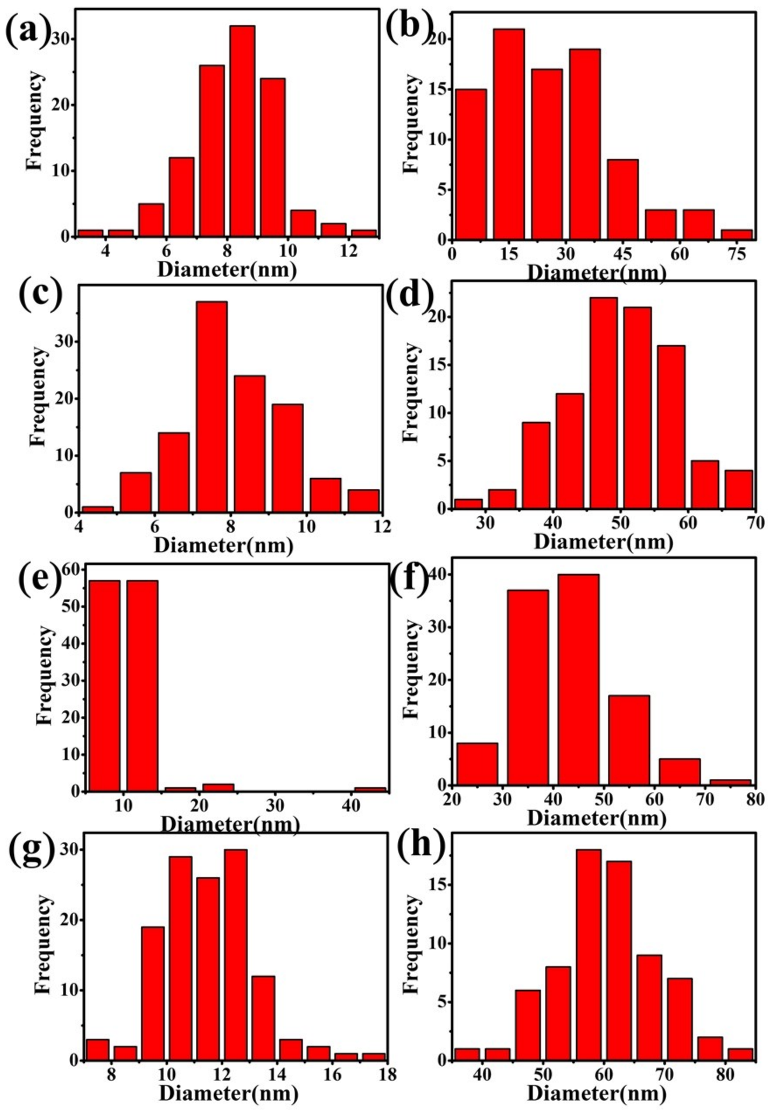

Fig. S5 Ag NPs size-distribution histograms of on the surface of TCFR@Ag-x nanospheres prepared with different silver contents: TCFR@Ag-0.1 (a), TCFR@Ag-3 (c), TCFR@Ag-10 (e), three samples were treated with NaOH for 22 h; and TCFR@Ag-3 (t=2 h) (g); The Ag core NPs size-distribution histograms of TCFR@Ag-x nanospheres: TCFR@Ag-0.1 (b), TCFR@Ag-3 (d), TCFR@Ag-10 (f), three samples were treated with NaOH for 22 h; and TCFR@Ag-3 (t=2 h) (h).

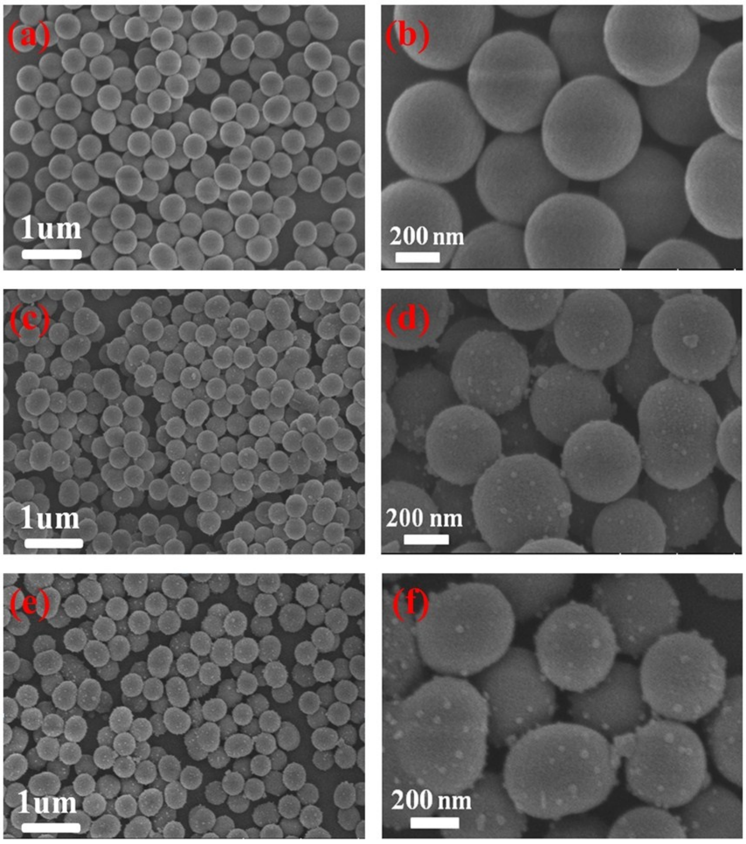

Fig. S6 SEM images of CFR (a, b), CFR@Ag-3 (c, d), and TCFR@Ag-3 (e, f), respectively.

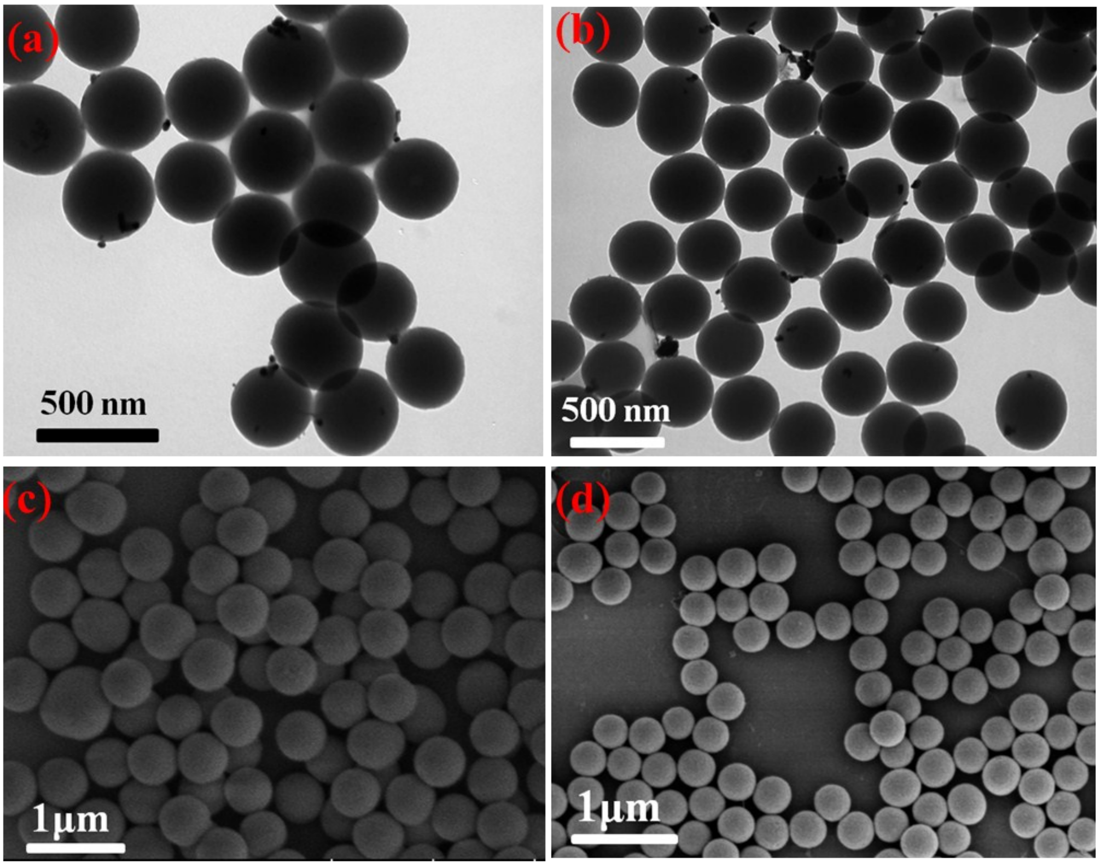

Fig. S7 TEM images of the carbonized CFR spheres treated with sodium hydroxide solution (a) and then loaded with silver NPs (b); SEM images of CFR (c) before and (d) after carbonizing.

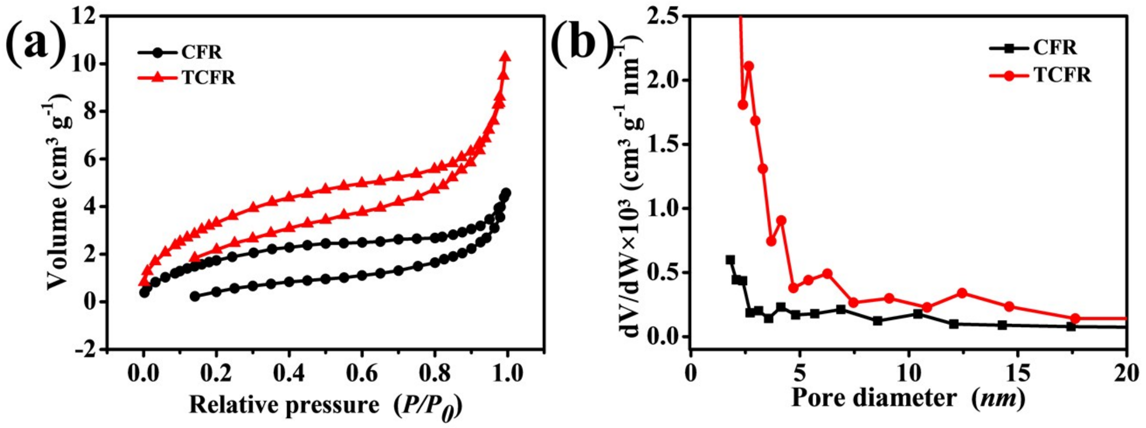

Fig. S8 (a) N_2 adsorption/desorption isotherms and (b) pore size distribution from Barret-Joyner-Hallender (BJH) desorption of CFR and TCFR.

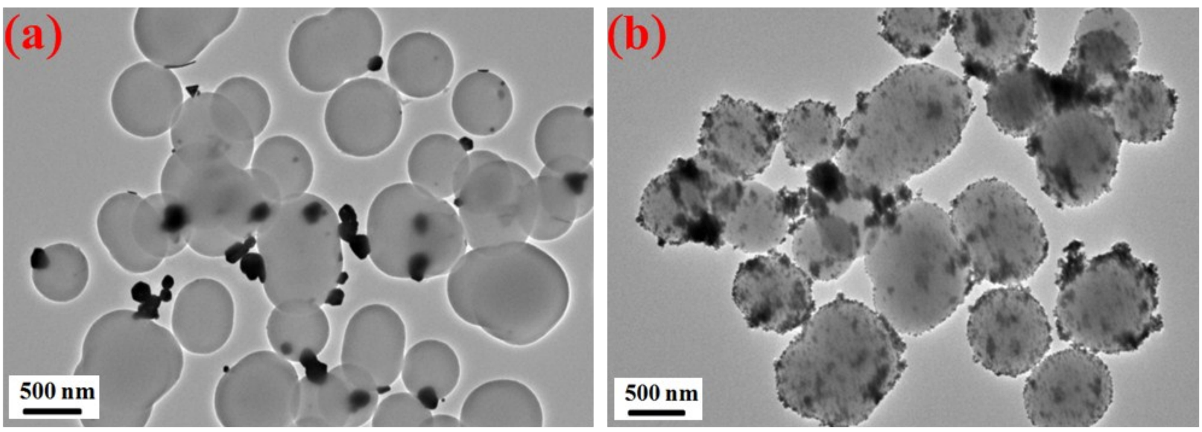

Fig. S9 TEM images of (a) TCFR@AuNPs and (b) TCFR@PdNPs.

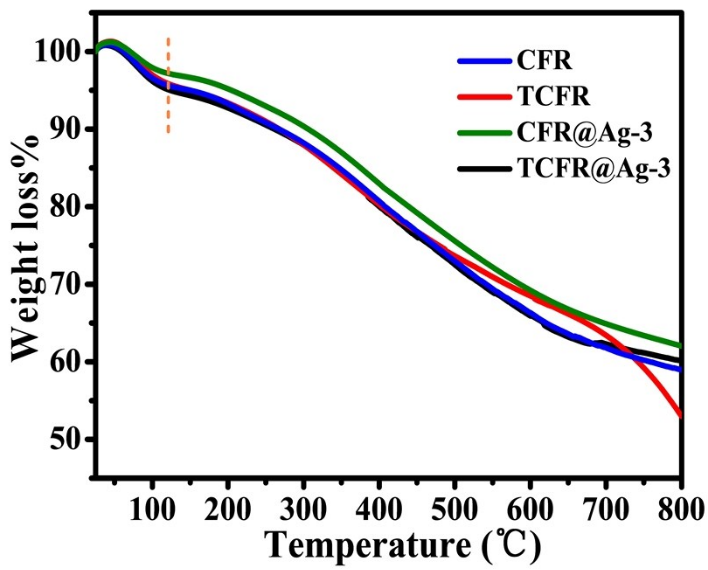

Fig. S10 TGA curves of CFR, TCFR, CFR@Ag-3, TCFR@Ag-3 under N_2 atmosphere.

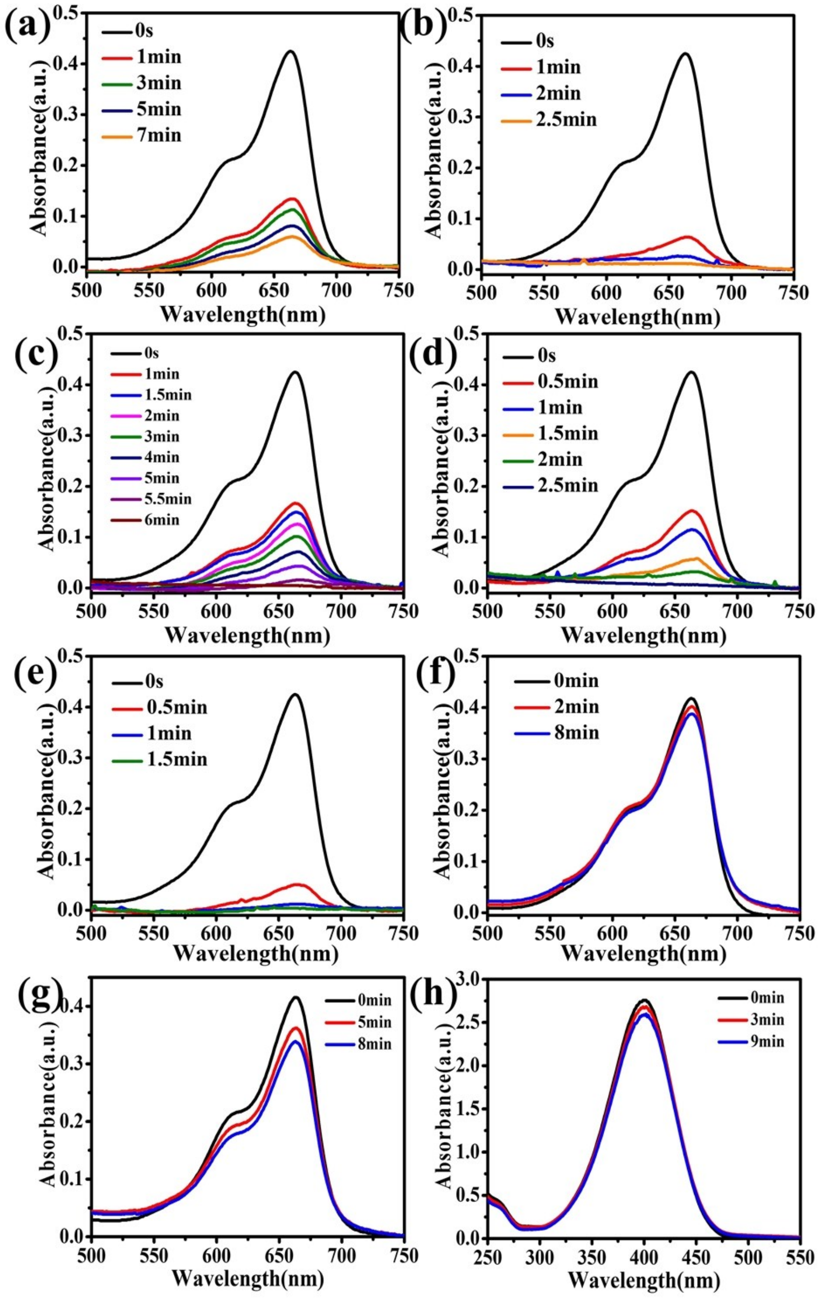

Fig. S11 UV-vis absorption spectra of the catalytic reduction of MB using catalysts: (a) CFR@Ag-0.5 (40 μL, 0.25 mg mL^{-1}), (b) CFR@Ag-10 (40 μL, 0.25 mg mL^{-1}), (c) TCFR@Ag-0.1 (40 μL, 0.25 mg mL^{-1}), (d) TCFR@Ag-10 (40 μL, 0.25 mg mL^{-1}), (e) TCFR@Ag-3(t=2 h) (40 μL, 0.25 mg mL^{-1}), (f) CFR (40 μL, 0.5 mg mL^{-1}), and (g) TCFR (40 μL, 0.5 mg mL^{-1}), 2.0 mL of 0.013 mM MB and 1.0 mL of 0.5 M $NaBH_4$ were used for the reduction of MB. (h) TCFR (80 μL, 0.5 mg mL^{-1}), 2.0 mL of 0.16 mM 4-NP and 1.0 mL of 0.2 M $NaBH_4$ were used for the reduction of 4-NP.

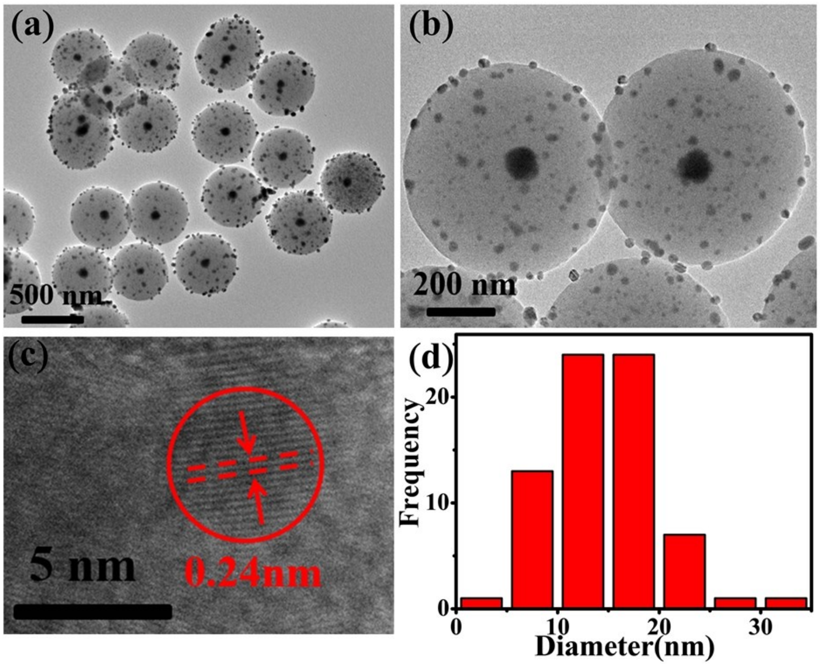

Fig. S12 TEM images (a, b), high-resolution TEM image (c) and size-distribution histogram (d) of TCFR@Ag-3 catalyst after six catalytic cycles.

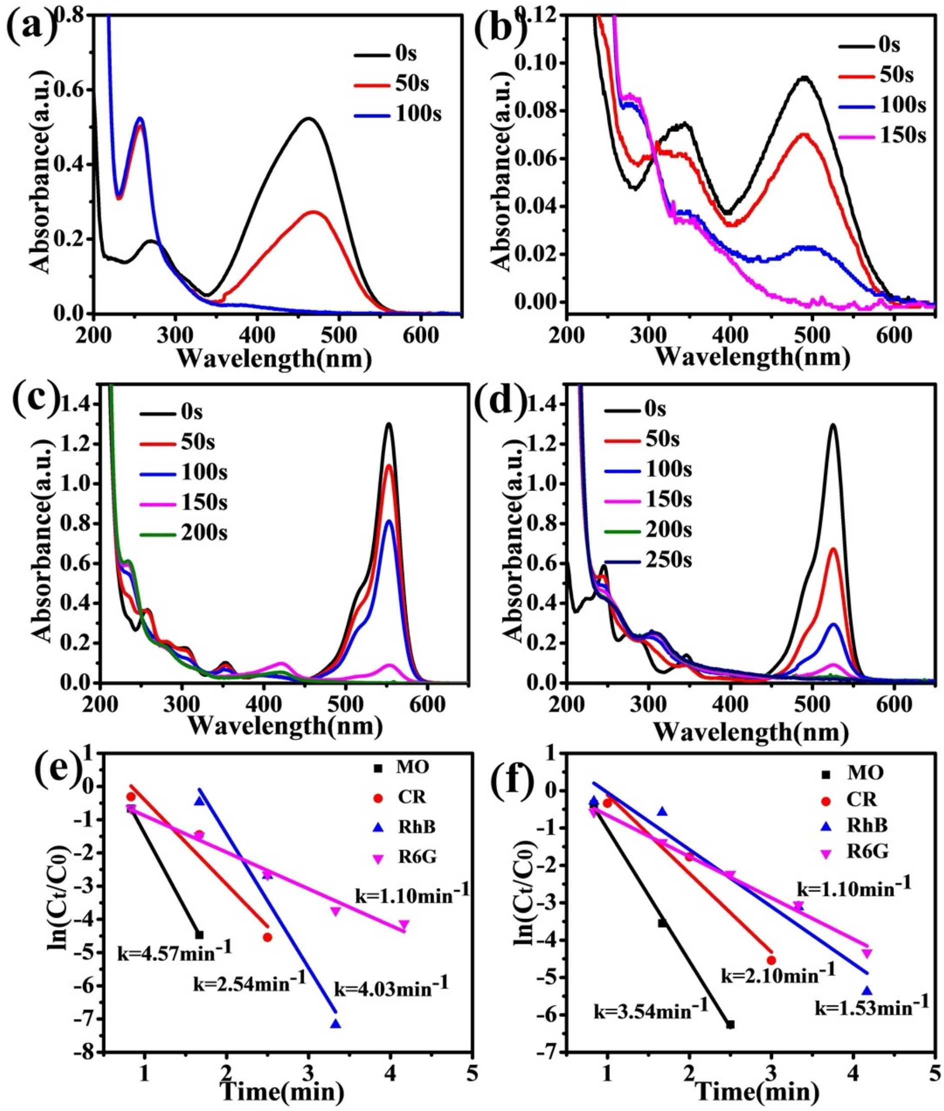

Fig. S13 Time-dependent UV-vis spectra of the reaction mixtures containing (a) MO, (b) CR, (c) RhB and (d) R6G aqueous solutions with the addition of $NaBH_4$ and CFR@Ag-3 (40 μL, 0.25 mg mL^{-1}) as a catalyst. Reaction conditions: 2.0 mL of 10 mg L^{-1} MO, CR, RhB and R6G and 1.0 mL of 0.5 M $NaBH_4$. (e) ln (C_t/C_0) vs. reaction time (t) plots for the reduction of four different dyes catalyzed by CFR@Ag-3 (40 μL, 0.25 mg mL^{-1}). (f) ln (C_t/C_0) vs. reaction time (t) plots for the reduction of four different dyes catalyzed by TCFR@Ag-3 (40 μL, 0.25 mg mL^{-1}).

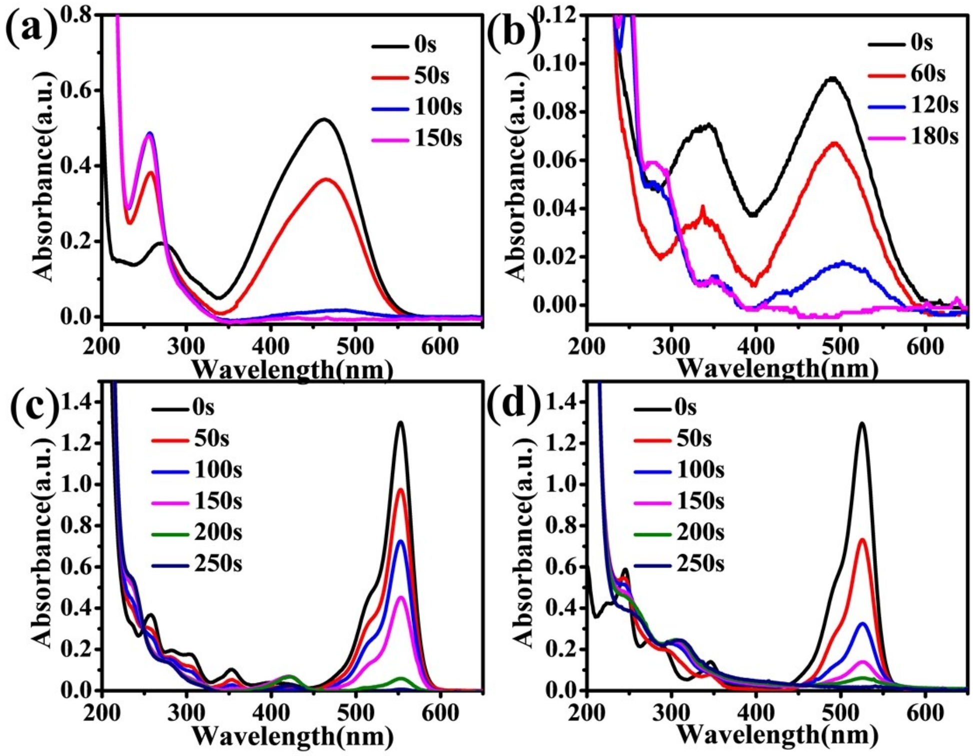

Fig. S14 Time-dependent UV-vis spectra of the reaction mixtures containing (a) MO, (b) CR, (c) RhB and (d) R6G aqueous solutions with the addition of $NaBH_4$ and TCFR@Ag-3 (40 μL, 0.25 mg mL^{-1}) as a catalyst. Reaction conditions: 2.0 mL of 10 mg L^{-1} MO, CR, RhB and R6G and 1.0 mL of 0.5 M $NaBH_4$.

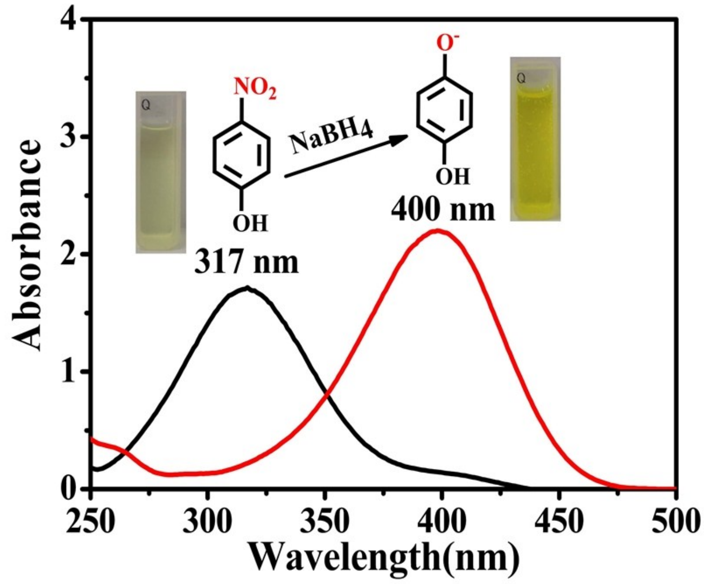

Fig. S15 UV-vis absorption spectra of 4-NP solution before and after adding $NaBH_4$.

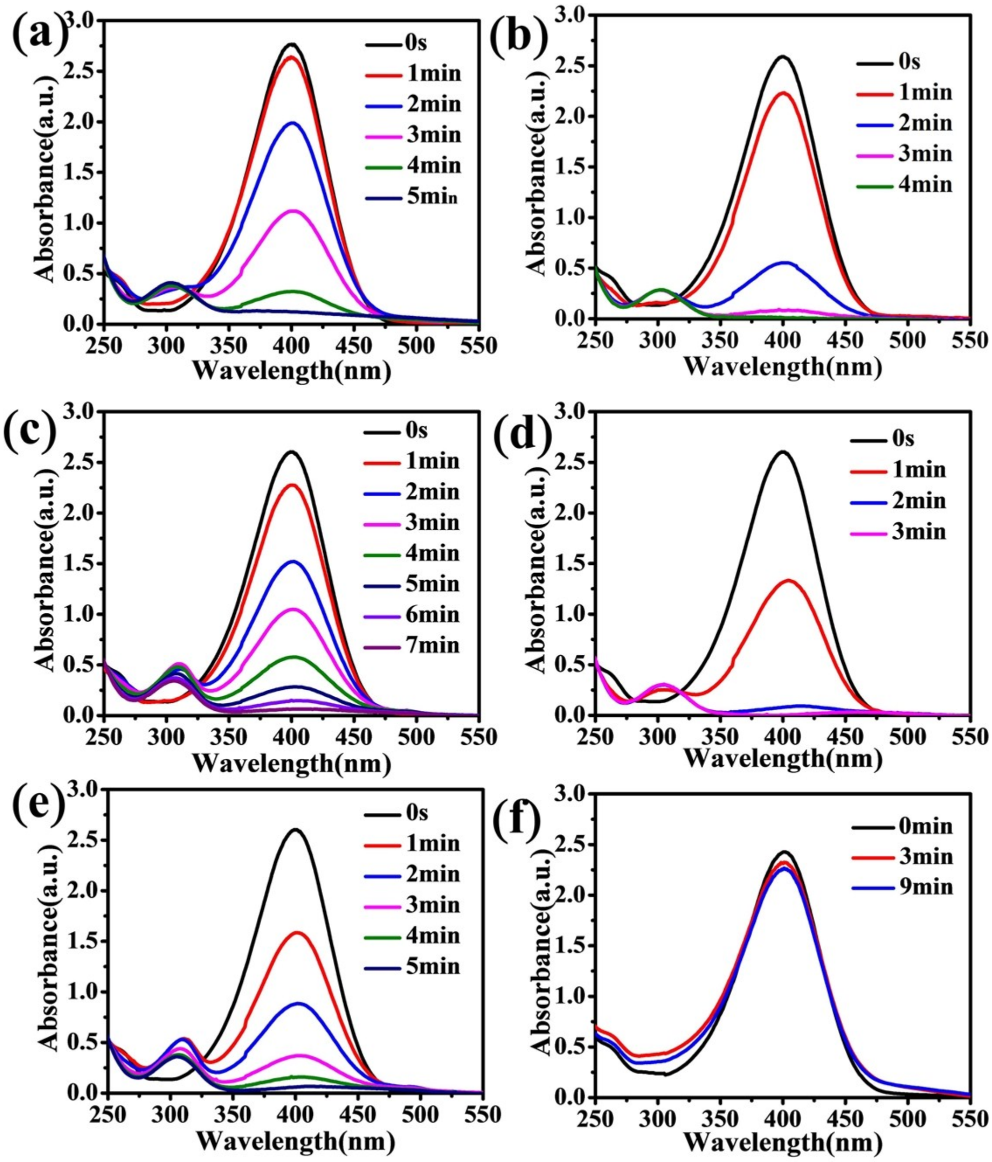

Fig. S16 Successive UV-vis spectra of the $NaBH_4$ reduction of 4-NP catalyzed by the catalysts: (a) CFR@Ag-0.5 (80 μL, 0.25 mg mL^{-1}), (b) CFR@Ag-10 (80 μL, 0.25 mg mL^{-1}), (c) TCFR@Ag-0.1 (80 μL, 0.25 mg mL^{-1}), and (d) TCFR@Ag-10 (80 μL, 0.25 mg mL^{-1}). (e) TCFR@Ag-3 (t=2 h) (80 μL, 0.25 mg mL^{-1}). (f) CFR (80 μL, 0.5 mg mL^{-1}) (2.0 mL of 0.16 mM 4-NP and 1.0 mL of 0.2 M $NaBH_4$ were used for the reduction of 4-NP).

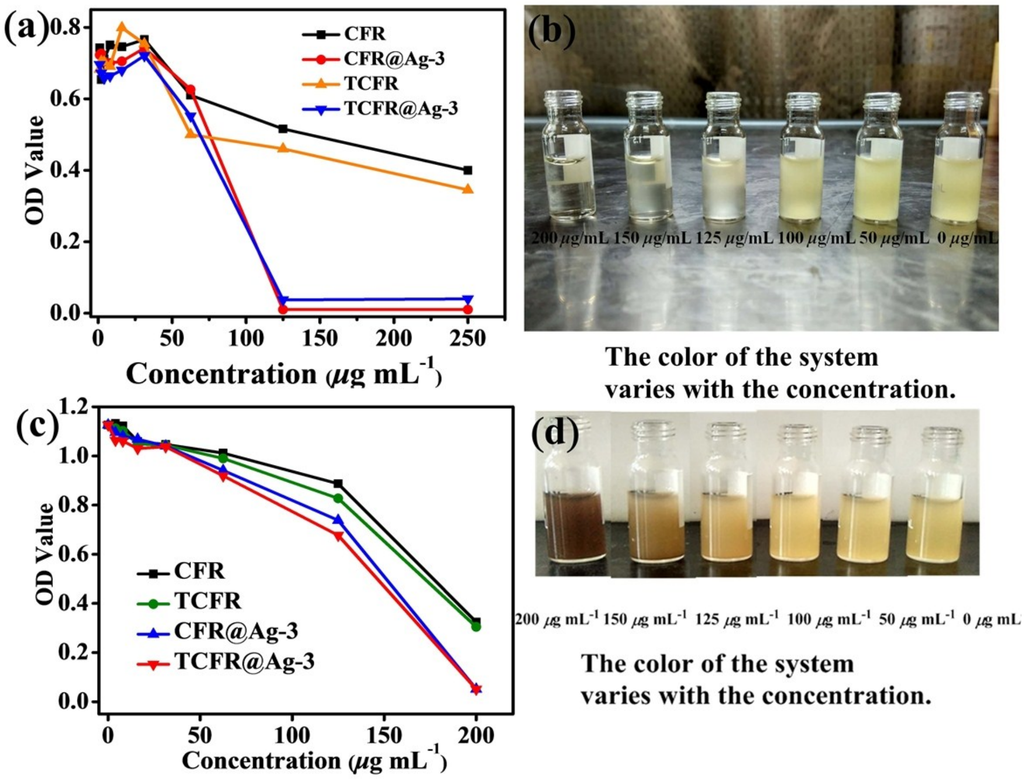

Fig. S17 The concentration influence of nanohybrids on the propagation of bacteria after incubation at 37 °C for 24 h against *E. coli* (a) and *S. aureus* (c). The *E. coli* (b) and *S. aureus* (d) solution color changes after the introduction of different concentrations of TCFR@Ag-3 antimicrobial materials.

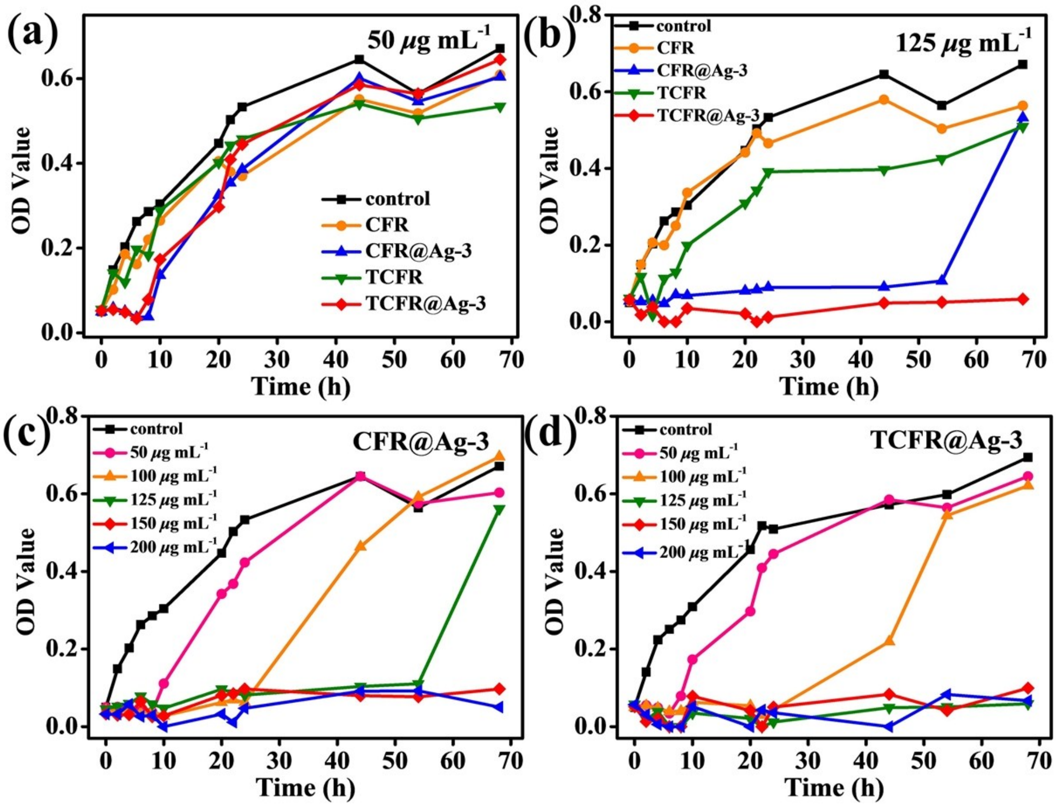

Fig. S18 Bacterial growth curves of *E. coli* (10^6 CFU mL^{-1}) after incubation at 37 °C for various durations with the sample concentration of (a) 50 μg mL^{-1} and (b) 125 μg mL^{-1}. Bacterial growth curves of *E. coli* (10^6 CFU mL^{-1}) after incubation at 37 °C for various durations with different concentration of CFR@Ag-3 (c) and TCFR@Ag-3 (d).

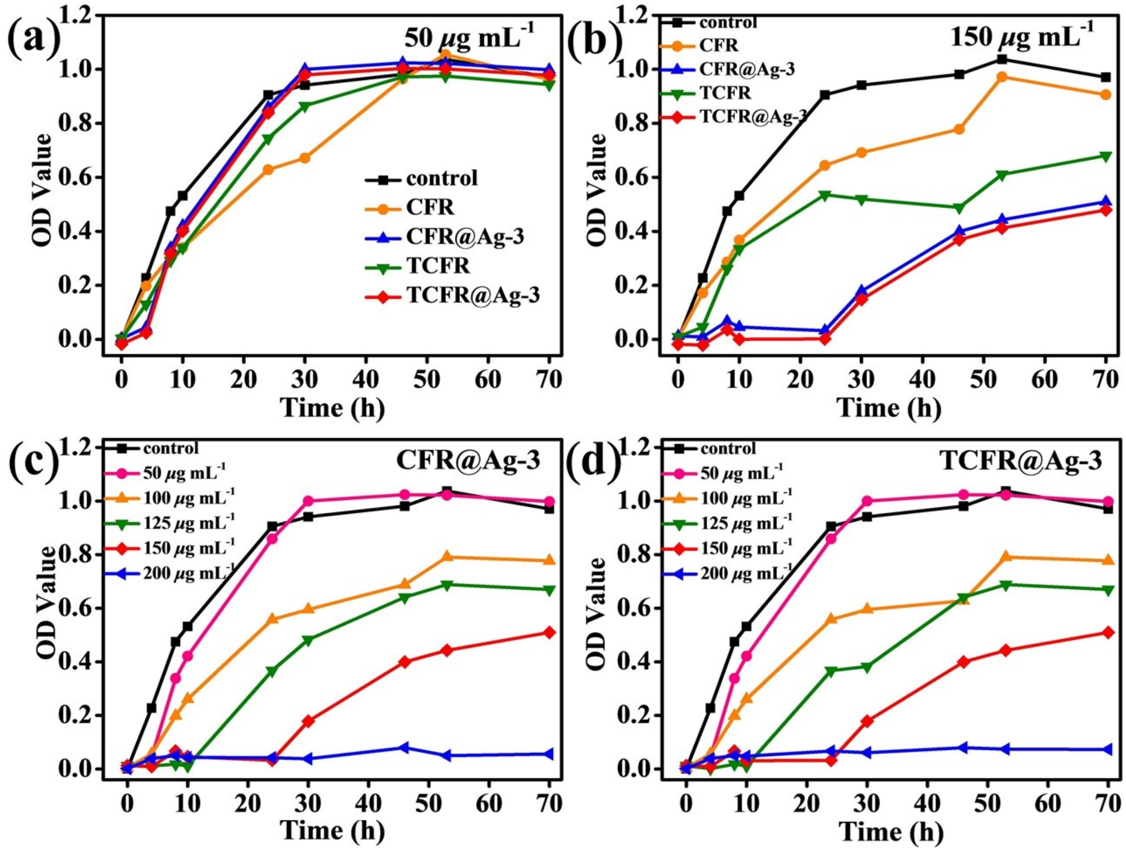

Fig. S19 Bacterial growth curves of *S. aureus* (10^6 CFU mL^{-1}) after incubation at 37 °C for various durations with the samples concentration of 50 μg mL^{-1} (a) and 150 μg mL^{-1} (b). Bacterial growth curves of *S. aureus* (10^6 CFU mL^{-1}) after incubation at 37 °C for various durations with different concentration of CFR@Ag-3 (c) and TCFR@Ag-3 (d).

Table S1. Synthesis parameters and properties of CFR nanospheres.

Sample		Catechol (g)	Formaldehyde solution (mL)	NH_3H_2O (mL)	Ethanol (mL)	Water (mL)	Temperature (℃)	Particle Size (nm)
CFR-1	Effect of	0.2	0.28	0.15	20	8	160	740±56
CFR-2	Catechol and	0.1	0.14	0.15	20	8	160	580±47
CFR-3	formaldehyde	0.05	0.07	0.15	20	8	160	510±48
CFR-4		0.1	0.14	0.15	28	0	160	-
CFR-5	Effect of	0.1	0.14	0.15	24	4	160	Irregular sphere
CFR-6	ethanol/ water	0.1	0.14	0.15	20	8	160	580±47
CFR-7	ratio	0.1	0.14	0.15	12	16	160	130±30
CFR-8		0.1	0.14	0.15	0	28	160	90±36
CFR-9		0.1	0.14	0.3	20	8	160	600±43
CFR-10	Effect of	0.1	0.14	0.15	20	8	160	580±47
CFR-11	$NH_3 \cdot H_2O$	0.1	0.14	0.1	20	8	160	-
CFR-12		0.1	0.14	0	20	8	160	-
CFR-13	Effect of	0.1	0.14	0.15	20	8	120	Irregular sphere
CFR-14	temperature	0.1	0.14	0.15	20	8	140	250±31
CFR-15		0.1	0.14	0.15	20	8	160	580±47

Table S2. Mesoscale properties of CFR and TCFR nanospheres.

Samples	BET surface area ($m^2\ g^{-1}$)	Pore volume ($cm^3\ g^{-1}$)	Pore size (nm)
CFR	7.17	0.0061	6.94
TCFR	13.28	0.0128	6.57

Table S3. Catalytic activity of different catalysts for the discoloration of MB and reduction of 4-NP.

Samples	Reaction conditions	Silver content (wt %)	Ag concentration (mol L^{-1})	Substrate	Time (min)	k (min^{-1})	TOF (h^{-1})
CFR@Ag-0.5	0.25 mg mL^{-1}, 40 μL	3.92	1.21×10^{-6}	MB	7.0	0.22	82
CFR@Ag-3	0.25 mg mL^{-1}, 40 μL	4.93	1.52×10^{-6}	MB	1.5	2.73	**1720**
CFR@Ag-10	0.25 mg mL^{-1}, 40 μL	5.97	1.84×10^{-6}	MB	2.5	1.37	339
TCFR@Ag-0.1	0.25 mg mL^{-1}, 40 μL	4.37	1.35×10^{-6}	MB	6.0	0.40	134
TCFR@Ag-3	0.25 mg mL^{-1}, 40 μL	4.74	1.46×10^{-6}	MB	1.0	1.23	**1933**
TCFR@Ag-10	0.25 mg mL^{-1}, 40 μL	10.79	3.33×10^{-6}	MB	2.5	4.67	633
CFR@Ag-0.5	0.25 mg mL^{-1}, 80 μL	3.92	2.42×10^{-6}	4-NP	5.0	0.79	496
CFR@Ag-3	0.25 mg mL^{-1}, 80 μL	4.93	3.04×10^{-6}	4-NP	4.0	1.12	**759**
CFR@Ag-10	0.25 mg mL^{-1}, 80 μL	5.97	3.68×10^{-6}	4-NP	4.0	1.76	407
TCFR@Ag-0.1	0.25 mg mL^{-1}, 80 μL	4.37	2.70×10^{-6}	4-NP	7.0	0.54	317
TCFR@Ag-3	0.25 mg mL^{-1}, 80 μL	4.74	2.92×10^{-6}	4-NP	4.0	1.12	**1338**
TCFR@Ag-10	0.25 mg mL^{-1}, 80 μL	10.79	6.66×10^{-6}	4-NP	3.0	3.24	300

Table S4. Comparison of the ability of various nanocatalysts for catalyzing the reduction of MB.

Samples	MB	Catalyst	Time (s) [a]	k (min^{-1}) [b]	TOF (h^{-1}) [c]	Refs
Fe_3O_4@PDA-Ag	2 mL, 4 mg L^{-1}	5.0 mg	540	0.43	-	1
Ag/Fe_3O_4@C	18 mL, 6 ×10^{-5} M	20 mg	600	0.34	-	2
urchin-like Fe_3O_4@PDA-Ag	10 mL, 40 mg L^{-1}	5.0 mg	240	1.78	-	3
cellulose supported silver nanoparticles	10 mg	1.0 mg	3600	0.04	-	4
MOF@Ag	1 mL, 5 × 10^{-5} M	0.5 mL, 0.5 mg mL^{-1}, 19 wt%	360	0.37	1.1	5
Pd-TNPs/RGO	2 mL, 5 × 10^{-5} M	5 μL,0.4 g L^{-1}, 59.2 wt%	420	0.4	73.6	6
AgNPs-Fe_3O_4@PDA	20 mL ,7.5 mg L^{-1}	5.0 mg	1800	0.09	-	7
CFR@Ag-3	1.04 × 10^{-5} M	0.25 mg mL^{-1},40 μL, 4.93 wt %	90	1.37	**1720**	This work
TCFR@Ag-3	1.04 × 10^{-5} M	0.25 mg mL^{-1},40 μL, 4.74 wt %	60	4.67	**1933**	This work

[a]The reduction time of MB in the presence of catalyst. [b]Apparent rate constant. [c]Turnover frequency (TOF) is defined as the number of moles of MB reduced per mole of Pd catalyst per hour.

Table S5. Comparison of the ability of various nanocatalysts for catalyzing the reduction of 4-NP.

Samples	4-NP (mol L^{-1})	catalyst	Time (min) [a]	k (min^{-1}) [b]	TOF (h^{-1}) [c]	Refs
Fe_3O_4/PDA@Ag	1.75×10^{-4}	1.0 mg L^{-1}, 1.0 mL, 11 wt %	5	0.60	41.2	8
Ag/GO-Dopa	5×10^{-5}	9 µL, (0.05 wt %, 0.5 mol %)	8	0.36	876	9
Fe_3O_4@RF-Ag	5×10^{-5}	10 mg L^{-1}, 7.44 wt %	6	0.68	-	10
RGO/Fe_3O_4/Ag	2 mL, 10.0 mM	7.4 mg, 14.52 wt %	4	0.68	30	11
SBA-15/$PDA_{0.6}$/Ag	200 µL, 20 mM	40 µL, 0.5 mg mL^{-1}, 3.24 wt %	7	0.89	571.2	12
PSS/Fe_3O_4/Ag	1mL, 10.0 mM	5.0 mg	12	0.15	-	13
Fe_3O_4@PPy-MAA/Ag	25 mL, 1 mmol	7.5 mg, 28.3 wt %	25	0.14	3.1	14
Au-PDA/RGO	2.7 mL, 0.1 mM	30 µL, 2 mg mL^{-1}	16	0.01	42	15
Ag-Au-rGO	2.8 mL, 5 mM	0.1 mg	6	0.21	152	16
RGO/Ag	1.5 mL,0.2 mM	0.1 mL, 10 mg mL^{-1}, 54.2 wt%	15	0.44	0.24	17
Ag^0@CMP	10 mL,10 mmol L^{-1}	7.4 mg, 0.5 mol % loading of Ag, 0.73 wt %		0.08	71.4	18
CFR@Ag-3	1.0×10^{-4}	0.25 mg mL^{-1},80 µL,4.93 wt %	4	1.12	**759**	This work
TCFR@Ag-3	1.0×10^{-4}	0.25 mg mL^{-1},80 µL, 4.74 wt %	4	1.12	**1338**	This work

[a]The reduction time of 4-NP in the presence of catalyst. [b]Apparent rate constant. [c]Turnover frequency (TOF) is defined as the number of moles of 4-NP reduced per mole of Pd catalyst per hour.

The TOF values of the catalytic reactions for MB were calculated according to the following equation:[19]

$$TOF = \frac{[MB] \times conversion}{[Ag] \times t}$$

The molar concentration [MB] of substrate was fixed to be 1.04×10^{-5} M. The Ag molar concentration [Ag] of CFR@Ag and TCFR@Ag were calculated and listed in Table S5 by ICP-AES. The TOF values of the catalytic reactions for 4-nitrophenol were calculated according to the equation similarly to MB. The molar concentration [4-NP] of substrate was 1.0×10^{-4} M. The Ag molar concentration [Ag] of CFR@Ag and TCFR@Ag were also calculated and listed Table S5.

References

1. Y. Xie, B. Yan, H. Xu, J. Chen, Q. Liu, Y. Deng and H. Zeng, *ACS Appl. Mater. Interfaces,* 2014, **6**, 8845-8852.
2. M. Zhu, C. Wang, D. Meng and G. Diao, *J. Mater. Chem. A,* 2013, **1**, 2118-2125.
3. K. Cui, B. Yan, Y. Xie, H. Qian, X. Wang, Q. Huang, Y. He, S. Jin and H. Zeng, *J. Hazard. Mater.*, 2018, **350**, 66-75.
4. M. Goswami, D. Baruaha and A. M. Das, *New J. Chem.,* 2018, **42**, 10868-10878.
5. A. Lajevardi, M. T. Yaraki, A. Masjedi, A. Nouri and M. H. Sadr, *J. Mol. Liq.*, 2019, **276**, 371-378.
6. G. T. Fu, L. Tao, M. Zhang, Y. Chen, Y. W. Tang, J. Lin and T. H. Lu, *Nanoscale*, 2013, **5**, 8007-8014.
7. M. Wu, Y. Li, R. Yue, X. Zhang and Y. Huang, *Sci. Rep.,* 2017, **7**, 42773.
8. B. Mao, Q. An, B. Zhai, Z. Xiao and S. Zhai, *RSC Adv*., 2016, **6**, 47761-47770.
9. E. K. Jeon, E. Seo, E. Lee, W. Lee, M. K. Um and B. S. Kim, *Chem. Commun*., 2013, **49**, 3392-3394.
10. Y. Zhong, Y. Ni, S. Li and M. Wang, *RSC Adv*., 2016, **6**, 15831-15837.
11. Z. Ji, X. Shen, X. Yue, H. Zhou, J. Yang, Y. Wang and L. Ma, *J. Colloid. Interf. Sci.,* 2015, **459**, 79-85.
12. Y. Song, H. Jiang, B. Wang, Y. Kong and J. Chen, *ACS Appl. Mater. Interfaces*, 2018, **10**, 1792-1801.
13. N. Li, Z. Ji, L. Chen, X. Shen, Y. Zhang, S. Chen and H. Zhou, *Appl. Surf. Sci.,* 2018, **462**, 1-7.
14. R. Dasa, V. S. Sypua, H. K. Paumoa, M. Bhaumika, V. Maharajb and A. Maity, *Appl. Catal. B*, 2019, **244**, 546-558.
15. W. Ye, J. Yu, Y. Zhou. D. Gao, D. Wang, C. Wang and D. Xue, *Appl. Catal. B*, 2016, **181**, 371-378.
16. K. Hareesh, R. P. Joshi, D. V. Sunith, V. N. Bhoraskar and S. D. Dholea, *Appl. Surf. Sci*., 2016, **389**, 1050-1055.
17. Y. Tian, Y. Cao, F. Pang, G. Chen and Xiao Zhang, *RSC Adv*., 2014, **4**, 43204-43211.
18. H. L. Cao, H. B. Huang, Z. Chen, B. Karadeniz, J. Lü and R. Cao, *ACS Appl. Mater. Interfaces*, 2017, **9**, 5231-5236.
19. X. Liu, F. Cheng, Y. Liu, H. Ji and Y. Chen, *J. Mater. Chem.*, **2010**, 20, 360-368.